

Soft x-ray photoemission studies of the HfO₂/SiO₂/Si system

S. Sayan, E. Garfunkel, and S. Suzer

Citation: *Appl. Phys. Lett.* **80**, 2135 (2002); doi: 10.1063/1.1450049

View online: <http://dx.doi.org/10.1063/1.1450049>

View Table of Contents: <http://apl.aip.org/resource/1/APPLAB/v80/i12>

Published by the [American Institute of Physics](#).

Related Articles

Stoichiometry dependence and thermal stability of conducting NdGaO₃/SrTiO₃ heterointerfaces
Appl. Phys. Lett. **102**, 071601 (2013)

Photoelectron spectroscopic study of band alignment of polymer/ZnO photovoltaic device structure
Appl. Phys. Lett. **102**, 043302 (2013)

Photoelectron spectroscopic study of band alignment of polymer/ZnO photovoltaic device structure
APL: Org. Electron. Photonics **6**, 17 (2013)

A possible origin of core-level shift in SiO₂/Si stacks
Appl. Phys. Lett. **102**, 041603 (2013)

Reexamination of band offset transitivity employing oxide heterojunctions
Appl. Phys. Lett. **102**, 031605 (2013)

Additional information on *Appl. Phys. Lett.*

Journal Homepage: <http://apl.aip.org/>

Journal Information: http://apl.aip.org/about/about_the_journal

Top downloads: http://apl.aip.org/features/most_downloaded

Information for Authors: <http://apl.aip.org/authors>

ADVERTISEMENT

AIP | Applied Physics
Letters

SURFACES AND INTERFACES
Focusing on physical, chemical, biological, structural, optical, magnetic and electrical properties of surfaces and interfaces, and more...

ENERGY CONVERSION AND STORAGE
Focusing on all aspects of static and dynamic energy conversion, energy storage, photovoltaics, solar fuels, batteries, capacitors, thermoelectrics, and more...

EXPLORE WHAT'S NEW IN APL

SUBMIT YOUR PAPER NOW!

Soft x-ray photoemission studies of the HfO₂/SiO₂/Si system

S. Sayan and E. Garfunkel^{a)}

Department of Chemistry, Rutgers University, Piscataway, New Jersey 08854

S. Suzer

Department of Chemistry, Bilkent University, 06533 Ankara, Turkey

(Received 8 March 2001; accepted for publication 19 December 2001)

Soft x-ray photoelectron spectroscopy with synchrotron radiation was employed to study the valence-band offsets for the HfO₂/SiO₂/Si and HfO₂/SiO_xN_y/Si systems. We obtained a valence-band offset difference of -1.05 ± 0.1 eV between HfO₂ (in HfO₂/15 Å SiO₂/Si) and SiO₂ (in 15 Å SiO₂/Si). There is no measurable difference between the HfO₂ valence-band maximum positions of the HfO₂/10 Å SiO_xN_y/Si and HfO₂/15 Å SiO₂/Si systems. © 2002 American Institute of Physics. [DOI: 10.1063/1.1450049]

The continuous shrinkage of complementary metal–oxide–semiconductor (CMOS) dimensions (now below 0.1 μm) to achieve higher performance and integration necessitates an increase in gate capacitance while maintaining low leakage current levels. The increased capacitance need is driving extensive research into the use of alternative gate insulators with a higher dielectric constant (ϵ_k) than that of SiO₂ ($\epsilon_k = 3.9$).^{1,2} The gate dielectric must form a high-quality low-defect-density interface with silicon. When high- ϵ_k materials such as ZrO₂, HfO₂, etc., are bonded directly to silicon they present higher interface state densities than are observed in the SiO₂/Si system. To overcome this problem, it is preferred to have a few monolayers of SiO₂ serving as a low-defect-density bottom oxide between the high- ϵ_k dielectric film and the silicon. Although this serves to decrease the interface state density, the capacitance also drops because of the low dielectric constant of SiO₂. Another requirement for any dielectric is that the barrier heights for electron and hole injection should be at least 1 eV (and preferably larger) to have sufficiently low leakage currents. It is, therefore, important to understand and control the band alignments of alternative dielectrics on silicon and on SiO₂. Photoemission is one of the most reliable methods to study these systems. Several high- ϵ_k materials are now being considered as replacement dielectrics including HfO₂, ZrO₂, Y₂O₃, and La₂O₃, as well as their silicates and aluminates. In particular, considerable attention is paid to HfO₂ due to its high dielectric constant ($\epsilon_k = 16$ –45),^{3,4} high resistivity, and high thermal stability.⁵

Recently, S. Miyazaki used high-resolution photoemission to study the valence-band offsets as well as work functions of ZrO₂, Al₂O₃, and Ta₂O₅ using total photoelectron yield spectroscopy.⁶ They calculated the band gaps using the measured band-offset and work-function values. Lucovsky and co-workers studied band offsets for ultrathin SiO₂ and Si₃N₄ films on Si(111) and Si(100) using soft x-ray photoemission spectroscopy (XPS).⁷ They have found that their spectrum in the valence-band-edge region was well modeled by a pair of Gaussian-broadened Fermi functions. They ob-

tained band offsets of 4.54 ± 0.1 eV for SiO₂/Si(100) with film thicknesses in the range of 8–12 Å. Hattori⁸ studied the SiO₂/Si system with different thickness (5–15 Å) regimes using high-resolution XPS. Both thickness and angle-resolved analytical procedures were used for analysis of the valence-band spectra. During the analysis, it was assumed that the density of states near the valence-band edge follows a parabolic energy dependence. Hattori reported that the top of the valence band of the oxide surface increased by about 0.2 eV near the thickness of 9 Å, which was attributed to oxidation-induced stress in the interfacial transition layer. In this contribution, we report on the valence-band alignments of HfO₂/10 Å SiO_xN_y/Si, HfO₂/15 Å SiO₂/Si and SiO₂/Si using soft x-ray photoemission.

HfO₂ films were deposited using chemical-vapor deposition (CVD) employing Hf-*t*-butoxide as the precursor on different substrates at ~ 400 °C. The substrate used was *p*-type Si(100) with a doping concentration of $\sim 1 \times 10^{15}$ cm⁻³. The thickness of the thermal SiO₂ was 15 Å and that of SiO_xN_y was 10 Å, as measured by medium energy ion scattering (MEIS). In the oxynitride, the O:N ratio was $\sim 4:1$. The soft x-ray measurements were performed at Brookhaven National Laboratories (BNL) on the U8B line using 120–400 eV photon energies. The spectra at the valence-band edges were modeled by Boltzmann-broadened step functions. We employed several methods to determine the valence-band edge.

The growth, materials, and dielectric properties of the films used in this study are described in more detail elsewhere.¹⁰ The dielectric constant of the HfO₂ thin films with Pt electrodes used here was determined to be ~ 26 after plotting the optical thickness of a series of HfO₂ films of different thicknesses on the 10 Å SiO_xN_y/Si substrate versus the electrical thickness as determined by the capacitances at accumulation. The leakage current densities were determined at 1 V beyond the flatband voltage in the inversion regime and found to be on the order of $\sim 10^{-7}$ A/cm² for the thinnest sample ($t_{qm} = 11.6$ Å).

We modeled the spectra at the valence-band edges by Boltzmann-broadened step functions. Different fitting functions and simple smoothing of the data do not measurably change the results; what is important is to have an accurate

^{a)}Electronic mail: garf@rutchem.rutgers.edu

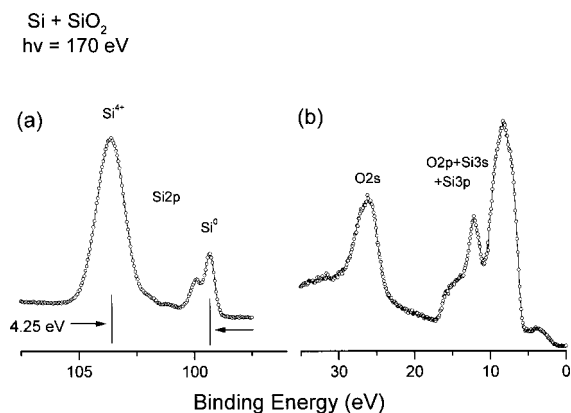


FIG. 1. Photoemission spectra corresponding to (a) the Si $2p$ core level of $10 \text{ \AA} \text{ SiO}_2/\text{Si}(100)$, and (b) the corresponding valence-band edge.

fit to the data in the high-energy-tail region (closest to the Fermi energy). Different methods have been reported to determine the “valence-band edge.” One method (M1) defines an energy based on the energy at the inflection point of a “best-fit” function. Another method (M2) employs a “best” straight-line fit to represent the decay in valence-band photoemission, and the point of intersection of this line with the base line is taken to be the valence-band edge⁶ (a related method combining M1 and M2 takes the tangent from the inflection point). We also present a third method (M3), somewhat similar to the one used in Ref. 7. The idea is to take as the energy edge the point where the signal rises above the base line by a certain fraction or percentage (e.g. 1–3%) indicating a measurable density of states. As we have no *a priori* knowledge of the electronic structure at the top of the valence band (the precise band structure is unknown, and even the similar ZrO_2 case is quite complex), nor any specific knowledge about a possible contribution from interface or defect states, this third method might be more appropriate in determining the electrical properties which rely on a knowledge of the experimental barrier heights (valence-band edges). It may be argued that a fitting procedure that includes the states lying close to the valence-band maximum is appropriate since the tunneling probability is a strong function of energy. A more complete description of the overall current leakage (both electron and hole) should integrate over the densities of states of the appropriate wave functions on each side of the barrier, have a better description of the barrier shape and height (hence, tunneling matrix element), as well as adding in other forms of charge transport.

Both the inflection point (M1) and the straight-line extrapolation (M2) methods underestimate the experimental band maximum positions, as the yield at the top of the valence band in our HfO_2 samples drops off slowly. The inflection point determination method is appealing for metals that have slowly varying density of states near the valence-band maximum. Methods 1 and 2 would introduce another uncertainty in locating the valence-band maximum since it will not provide a good description of the shape in the vicinity of the valence-band maximum and would vary with instrumental resolution. The specific shape of the valence band in the vicinity of its maximum is an intrinsic property of the system under investigation. Therefore, methods M1 and M2 may be less appropriate for wider band gap oxides⁹ where a single

TABLE I. Valence-band energies relative to the valence band of $\text{Si}(100)$ obtained by employing three different methods.

Sample	Method 1	Method 2	Method 3
$\text{Si}(100)$	$\Delta E_v(\text{eV})=0$	0.00	0.00
$\sim 10 \text{ \AA} \text{ SiO}_2$	$4.10 (\pm 0.02)$	$4.35 (\pm 0.05)$	$4.25 (\pm 0.07)$
$\sim 15 \text{ \AA} \text{ SiO}_2$	3.80	4.50	4.49
$\text{HfO}_2/10 \text{ \AA} \text{ SiO}_x\text{N}_y/\text{Si}$	3.03	3.63	3.44
$\text{HfO}_2/15 \text{ \AA} \text{ SiO}_2/\text{Si}$	3.03	3.63	3.44

value offset is needed. The valence-band offsets determined by the three methods are given in Table I. The nature of the methods employed translates into different valence-band offset values. The inflection point method underestimated the valence-band offsets, whereas the straight-line method overestimated the offset magnitudes. The data scatter in the spectra is relatively small, and the error associated with any given fitting procedure is significantly better than 100 meV. As the experimental and fitting error is small (listed in Table I), our main uncertainty in valence-band determination originates from the choice of the fitting procedure.

In addition to the HfO_2 films, we measured photoemission yield for the pure $\text{SiO}_2/\text{Si}(100)$ system at two different thicknesses. The valence-band offset of $\text{SiO}_2/\text{Si}(100)$ is modeled and found to be 4.25 eV (using M3) for a SiO_2 thickness of $\leq 10 \text{ \AA}$, in very good agreement with the literature.⁸ This value is also cross checked by the difference between the Si $2p$ core levels of Si and SiO_2 , since the difference in energy between the Si $2p$ core level and the valence-band maximum is essentially constant.¹¹ Figure 1(a) presents the spectrum for the Si $2p$ core level of $\sim 10 \text{ \AA} \text{ SiO}_2/\text{Si}(100)$. The energy separation between the metallic Si $2p_{3/2}$ and $\text{Si}^{4+} 2p_{3/2}$ is found to be 4.25 eV. The corresponding valence-band edges are given in Fig. 1(b). The valence-band offset is found to be 4.25 eV following the fitting procedure described above. The energy separation between the Si $2p$ core level and corresponding valence-band edge was constant at 98.5 eV. Valence-band offset values obtained for $\text{SiO}_2/\text{Si}(100)$ systems, using this method, are in good agreement with literature values. We are mainly interested in the difference in the valence-band edges to determine the offsets rather than the precise position of the valence-band edges.

The deconvolution of the Hf $4f$ spin-orbit couple is performed after a Shirley background subtraction, and the area ratio (3:4) of the couple and 1.65 eV splitting in energy are taken into consideration. The binding energy of Hf $4f_{7/2}$ is measured to be 17.9 eV, in agreement with the range of values given in the literature (16.7–18.1).^{12,13}

In order to account for the different extents of charging in thicker HfO_2 samples, the Hf $4f$ levels of known position are used as reference peaks, as they are sharp. In the case of $\sim 15 \text{ \AA} \text{ SiO}_2/\text{Si}(100)$, we took advantage of the constant separation in energy between the Si $2p$ core level and the valence-band maximum. This is also cross checked with the position of the $\text{Si}(100)$ valence-band edge measured in a separate run. The valence-band offset of SiO_2/Si is found to be 4.49 ± 0.1 . It is worth noting that we observed an ~ 0.24 eV increase in the valence-band maximum in the oxide for thicknesses of ~ 10 and $\sim 15 \text{ \AA}$, as in Ref. 8. In a separate

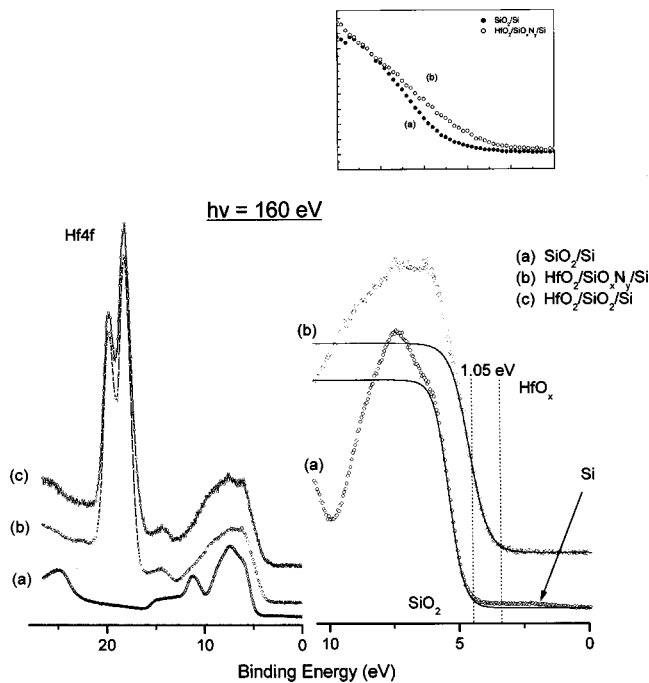


FIG. 2. Photoemission spectra of SiO_2/Si (a), $\text{HfO}_2/10 \text{ \AA} \text{SiO}_x\text{N}_y/\text{Si}$ (b), and $\text{HfO}_2/15 \text{ \AA} \text{SiO}_2/\text{Si}$ (c) systems. The right-hand panel of the figure displays our fitting procedure. In the upper-right hand, the inset shows an example of the difference of the photoemission yield at the top of the valence-band region. (The energy axis of one spectrum has been shifted, approximately 1 eV, to demonstrate the difference in shape in the vicinity of valence-band maximum.)

paper we will discuss energy referencing (to vacuum and Fermi levels), charging, initial state and final state effects, and band bending, all of which make energy-level determination complex.

It is important to note that the valence band of the $\text{HfO}_2/\text{SiO}_2/\text{Si}$ system (Fig. 2) presents an offset of $-1.05 \pm 0.1 \text{ eV}$ with respect to that of SiO_2/Si . Therefore, it can be inferred that the valence-band edge of HfO_2 lies within -1.05 eV of the valence-band edge of silicon dioxide. Recently, Robertson¹⁴ calculated the valence- and conduction-band offsets of various oxides on silicon. He reported valence-band-offset values of 4.4 and 3.4 eV for SiO_2/Si and HfO_2/Si , respectively. Accordingly, a valence-band offset of up to -1.0 eV can be expected for the $\text{HfO}_2/\text{SiO}_2$ system, in very good agreement with our findings.

The valence-band edges of $\text{HfO}_2/10 \text{ \AA} \text{SiO}_x\text{N}_y/\text{Si}$ and $\text{HfO}_2/15 \text{ \AA} \text{SiO}_2/\text{Si}$ were found to be at the same position (Fig. 2). Hence, nitrogen incorporation in this oxynitride does not seem to affect the valence-band position, at least within the level given by our experimental resolution and fitting procedure. The intensity differences in the valence-band region can be attributed to the difference in nitrogen incorporation in the bottom oxide.

The determined valence-band offsets for the systems studied here can be used to derive values for conduction-band offsets if the gap is known:

$$\Delta E_c(\text{HfO}_2 - \text{Si}) = E_g(\text{HfO}_2) + \Delta E_v(\text{SiO}_2 - \text{HfO}_2) - \Delta E_v(\text{SiO}_2 - \text{Si}) - E_g(\text{Si}). \quad (1)$$

We are cognizant that there is no consensus on the values to be used for the band gap of HfO_2 (or even the most reliable experimental method to determine the gap). If we choose a HfO_2 band gap of 5.7 eV, as has been suggested by some,¹ then the conduction-band offset becomes $\sim 1.2 \text{ eV}$ ($= 5.7 + 1.1 - 4.5 - 1.1 \text{ eV}$). Unfortunately, the uncertainty on this number is high, primarily because of uncertainties in the band gap (numbers above 6 eV have been reported). Even if the HfO_2 -Si conduction-band offset is of order 1 eV, tunneling will be less than a simple calculation would lead one to believe, since there are usually 1–2 ML of SiO_2 situated between the HfO_2 and Si. On-going photoemission, inverse photoemission, and other studies of ultrathin HfO_2 and other high- ϵ_k films ($\text{EOT} < 20 \text{ \AA}$) will help better understand these effects as well as determine band gaps and conduction-band offsets more accurately for these technologically critical material systems.

We have estimated the valence-band maximum of the systems under investigation using several different methods. The valence-band edges of $\text{HfO}_2/10 \text{ \AA} \text{SiO}_x\text{N}_y/\text{Si}$ and $\text{HfO}_2/15 \text{ \AA} \text{SiO}_2/\text{Si}$ were found to be at the same position within experimental error, inferring that nitrogen doping of the bottom oxide does not significantly change the position of the valence-band maximum. The valence band of $\text{HfO}_2/\text{SiO}_2/\text{Si}$ and $\text{HfO}_2/\text{SiO}_x\text{N}_y/\text{Si}$ systems present an offset of $-1.05 \pm 0.1 \text{ eV}$ with respect to that of SiO_2/Si .

The authors acknowledge the Semiconductor Research Corporation and the National Science Foundation for financial support. The authors would like to thank M. Banasak-Holl, F. R. McFeely, Glen Wilk, Evgeni Gusev, Ed Cartier, Gerry Lucovsky, V. Misra, R. Opila, and Jack Rowe for their help in various parts of this work.

¹G. D. Wilk, R. M. Wallace, and J. M. Anthony, *J. Appl. Phys.* **89**, 5243 (2001).

²A. I. Kingon, J.-P. Maria, and S. K. Streiffer, *Nature (London)* **406**, 1032 (2000).

³K. Kukli, J. Aarik, A. Aidla, H. Siimon, M. Ritala, and M. Leskela, *Appl. Surf. Sci.* **112**, 236 (1997).

⁴C. T. Hsu, Y. K. Su, and M. Yokoyama, *Jpn. J. Appl. Phys., Part 1* **31**, 2501 (1992).

⁵B. H. Lee, L. Kang, R. Nieh, W.-J. Qi, and J. C. Lee, *Appl. Phys. Lett.* **76**, 1926 (2000).

⁶S. Miyazaki, *J. Vac. Sci. Technol. B* **19**, 2212 (2001).

⁷J. W. Keister, J. E. Rowe, J. J. Kolodziej, H. Niimi, T. E. Madey, and G. Lucovsky, *J. Vac. Sci. Technol. B* **17**, 1831 (1999).

⁸Hattori, in *Fundamental Aspects of Ultrathin Dielectrics on Si-based Devices*, edited by E. Garfunkel, E. P. Gusev, and A. Y. Vul' (Kluwer Academic, Dordrecht, The Netherlands, 1998), pp. 241–256.

⁹E. A. Kraut, R. W. Grant, J. R. Waldrop, and S. P. Kowalczyk, *Phys. Rev. B* **28**, 1965 (1983).

¹⁰S. Sayan, S. Aravamudhan, B. W. Busch, H. W. Schulte, F. Cosandey, G. D. Wilk, T. Gustafson, and E. Garfunkel, *J. Vac. Sci. Technol. A* **20**, 507 (2002).

¹¹F. J. Himpsel, F. R. McFeely, A. Taleb-Ibrahimi, J. A. Yarmoff, and G. Hollinger, *Phys. Rev. B* **38**, 6084 (1988).

¹²D. D. Sarma and C. N. R. Rao, *J. Electron Spectrosc. Relat. Phenom.* **20**, 25 (1980).

¹³C. Morant, L. Galan, and J. M. Sanz, *Surf. Interface Anal.* **16**, 304 (1990).

¹⁴J. Robertson, *J. Vac. Sci. Technol. B* **18**, 1785 (2000).